Supplementary Information (SI) for Environmental Science: Nano.

Supplementary material

Facet-Dependent Hematite Reactivity in Cr(VI) Removal with Fe(II)

20 pages, 4 Texts, 2 Tables and 12 Figures

Text S1. Electrochemical testing of tafel polarization diagrams

As reported in the literature,[1,2] hematite samples were served as working electrodes. Specifically, the platinum working electrode was first pre-cleaned in acetone and used to support the substrate of the hematite samples. Then 20 μL of hematite suspension was added dropwise, and finally dried with an infrared lamp to form a dense hematite film on the surface of the Pt electrode. Tafel plots were obtained using a CHI-600C electrochemical workstation (Shanghai Chenghua, China) with a three-electrode configuration, comprising a platinum counter electrode and a saturated calomel reference electrode. The electrolyte was a 0.5 M Na_2SO_4 aqueous solution.

Text S2. Determination of Cr(VI) and Fe(II) concentration in the supernatant

Cr(VI) and Fe(II) was analyzed by 1,5-diphenylcarbonyldihydrazide method and 1,10-phenanthroline method, respectively. These methods are highly sensitive and the detection limits for Cr(VI) and Fe(II) are 0.01 and 0.5 μM, respectively.

For the analysis of Cr(VI), 1 mL of the solution was sampled and transferred into tubes containing 0.2 mL of 0.2 g/L 1,5-diphenylcarbonyldihydrazide solution, 0.1 mL of 0.12 M HCl for acidification, and 3.7 mL of ultrapure water. The samples were then thoroughly mixed to ensure complete reaction and incubated for 10 minutes to allow for optimal color development of the Cr(VI)-1,5-diphenylcarbonyldihydrazide complex. We observed that the complex formed was very stable after-color development.

For the analysis of Fe(II), 2.5 mL of the solution was sampled and transferred into tubes containing 0.5 mL of 2 g/L 1,10-phenanthroline with sodium acetate buffer adjusted to pH 4.1, and 2 mL of ultrapure water. The samples were then thoroughly mixed to ensure complete reaction and incubated for 10 minutes to allow for optimal color development of the Fe(II)-1,10-phenanthroline complex. We observed that the complex formed was very stable after color development.

The entire process from sampling to color development and measurement was rapid and efficient. Sampling itself took approximately 5 seconds. The samples were directly added to tubes containing the color developing agents, and the Cr(VI)/Fe(II) quickly formed a complex with the agent within 5 minutes. The complexes were very stable, allowing us to accumulate multiple samples and then move the samples outside the glovebox, and analyze them using UV-Vis spectrophotometry within 1 hour.

Text S3. Adsorption kinetics

The Fe(II) and Cr(VI) adsorption kinetic data were analyzed using pseudo-first-order and pseudo-second-order kinetic models.[3]

The pseudo-first-order kinetic model is given by the following equation:

$$log(q_e - q_t) = logq_e - \frac{k_1 t}{2.303} \quad (1)$$

The pseudo-second-order kinetic model is written as the following equation:

$$\frac{t}{q_t} = \frac{1}{k_2 q_e^2} + \frac{t}{q_e} \quad (2)$$

where q_e and q_t (μmol/g) are the uptake of Fe(II) or Cr(VI) by hematite at equilibrium and time t (min), k_1 and k_2 are the pseudo-first-order rate constant and pseudo-second-order rate constant for the adsorption process, respectively.

Text S4. Reduction kinetics

The initial phase lasts on the order of 30 minutes and is described by a second-order kinetic law:[4]

$$-\frac{d[Cr(VI)]}{dt} = k[Cr(VI)][Fe(II)] \quad (3)$$

For our experimental conditions [Fe(II)] is equal to [Cr(VI)], the integration yields:

$$[Cr(VI)]_t = \frac{[Cr(VI)]_0}{1 + k[Cr(VI)]_0 t} \quad (4)$$

where $[Cr(VI)]_0$ and $[Cr(VI)]_t$ are the initial and equilibrium concentrations of Cr(VI), respectively. k is the second-order rate constant for the redox process.

Table S1. Kinetic fitting parameters of pseudo-first-order and pseudo-second-order models for Fe(II) and Cr(VI) adsorption.

Hematite	pH	Fe(II)					Cr(VI)				
		q_e (μmol/g)	The·pseudo-first-order model		The·pseudo-second-order model		q_e (μmol/g)	The·pseudo-first-order model		The·pseudo-second-order model	
			k_1 (min^{-1})	R^2	k_2 (g/(μmol·min))	R^2		k_1 (min^{-1})	R^2	k_2 (g/(μmol·min))	R^2
HNPs	3	3.43	0.06	0.9356	0.29	0.9999	18.20	0.01	0.8878	0.05	0.9995
	5	23.36	0.05	0.9024	0.04	1.0000	8.71	0.01	0.8954	0.11	0.9992
	7	38.06	0.06	0.8125	0.03	1.0000	1.87	0.11	0.9647	0.53	0.9998
HNRs	3	2.67	0.15	0.8689	0.37	1.0000	23.14	0.01	0.8961	0.04	0.9992
	5	18.15	0.06	0.9457	0.05	1.0000	14.57	0.02	0.9185	0.07	0.9998
	7	28.99	0.08	0.9885	0.03	0.9999	6.11	0.11	0.8406	0.16	1.0000

Table S2. Comparison of maximum Fe(II) and Cr(VI) adsorption capacity of hematite with different exposed crystal facets under different pH conditions.

Hematite	pH	Fe(II)			Cr(VI)		
		q_e (μmol/g)	site density [a] (#Fe/nm²)	site density in {001} [b] or {110} [c] (#Fe/nm²)	q_e (μmol/g)	site density [a] (#Cr/nm²)	site density in {001} [b] or {110} [c] (#Cr/nm²)
HNPs	3	3.43	0.19	0.24	18.20	1.01	1.26
	5	23.36	1.29	1.61	8.71	0.48	0.60
	7	38.06	2.11	2.63	1.87	0.10	0.13
HNRs	3	2.67	0.20	0.27	23.14	1.72	3.13
	5	18.15	1.35	1.82	14.57	1.07	2.13
	7	28.99	2.15	2.86	6.11	0.45	1.03

a Site density=$(q_e \times 6.02 \times 10^{23})/(SSA \times 10^{18} \times 10^6)$, representing the number of Fe(II) or Cr(VI) atoms adsorbed per square nanometer.

b Site density in {001}=site density/80.18%.

c Site density in {110}=(site density-39.15%×site density in {001})/39.15%.

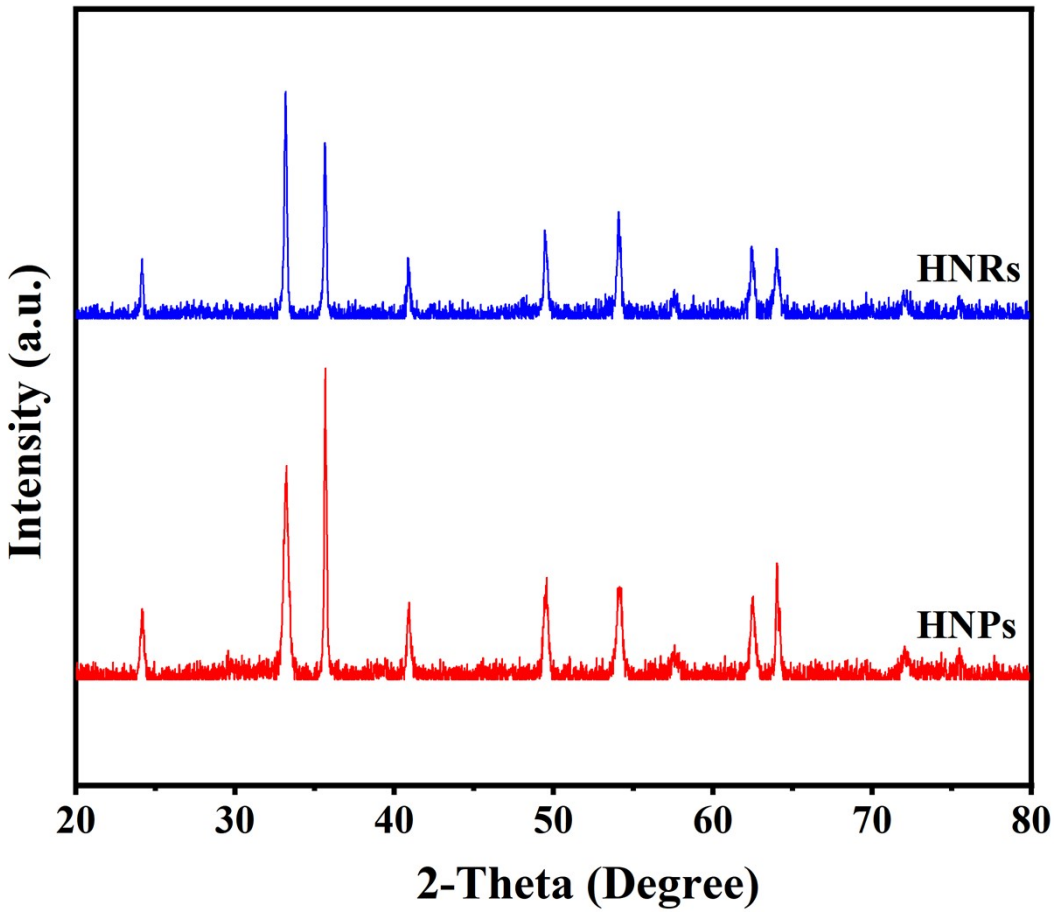

Fig. S1 Powder XRD patterns of HNPs and HNRs.

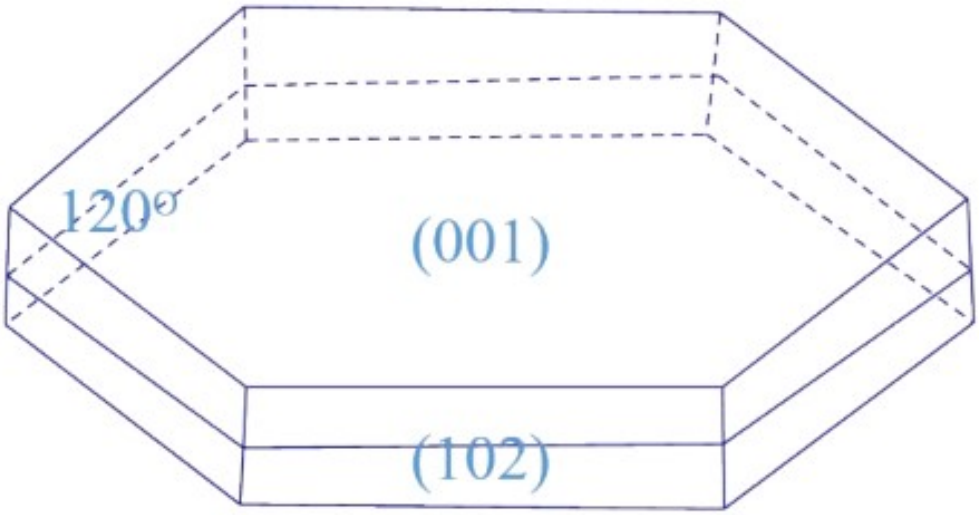

Fig.S2 Geometrical model of HNPs.

HNPs consist of two symmetric {001} facets on the basal planes and six equivalent {102} facets on the lateral surfaces. The average dimensions of these hexagonal nanoplates are 105.6 nm in side length and 22.6 nm in height. The relative abundance of the {001} and {102} facets, denoted as %S{001} and %S{102} respectively, was calculated using the following approach:

$$\%S\{001\}=\frac{\frac{3\sqrt{3}}{2}*105.6^2*2}{(\frac{3\sqrt{3}}{2}*105.6^2*2+105.6*22.6*6)}=80.18\% \quad (5)$$

$$\%S\{102\}=1-\%S\{001\}=19.82\% \quad (6)$$

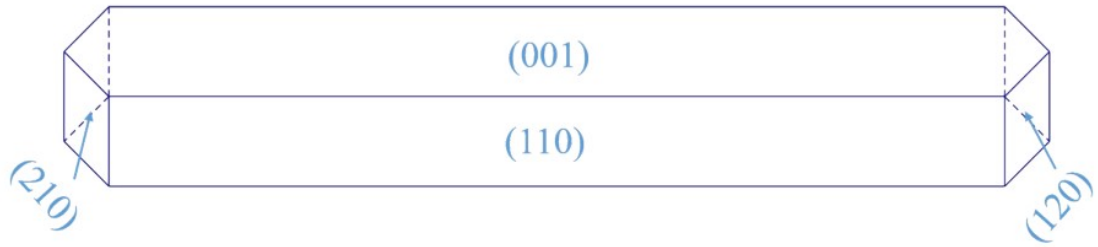

Fig.S3 Geometrical model of HNRs.

Hematite nanorods (HNRs) were characterized by the presence of two symmetric {001} facets on their basal planes and four lateral facets consisting of two equivalent {110} facets, two equivalent {120} facets, and two equivalent {210} facets. These nanorods exhibit a regular cylindrical morphology with dimensions of 416.7 nm in length, and 88.9 nm in both width and height. The relative surface abundances, denoted as %S{110}, %S{001}, and the combined %S{120}+{210}, were calculated using the following methodology:

%S{001}=%S{110}=

$$(416.7 * 88.89/(416.7 * 88.89 + \frac{\sqrt{3}}{2} * 88.89^2 + \frac{1}{2} * \frac{\sqrt{3}}{2} * 88.89^2))/2 = 39.15\% \quad (7)$$

%S{102}=%S{210}=(1-%S{001}- %S{110})/2=10.85% (8)

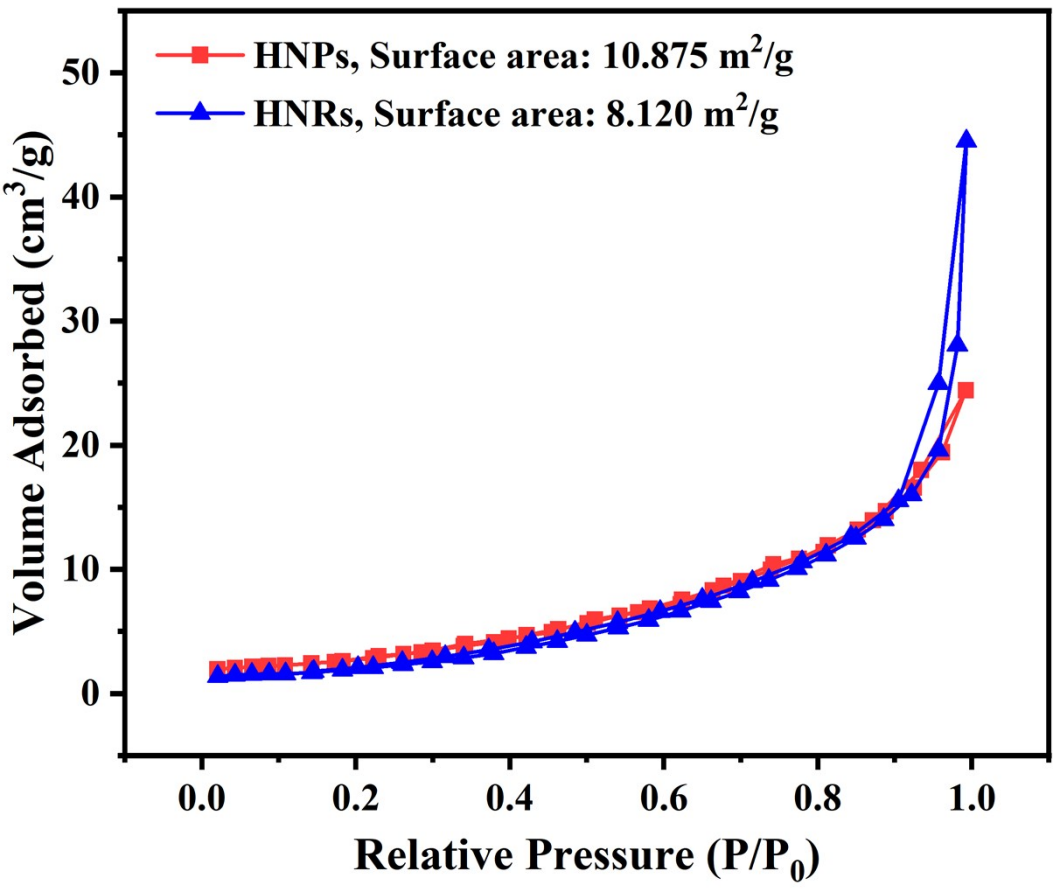

Fig. S4 Nitrogen adsorption and desorption isotherms of HNPs and HNRs.

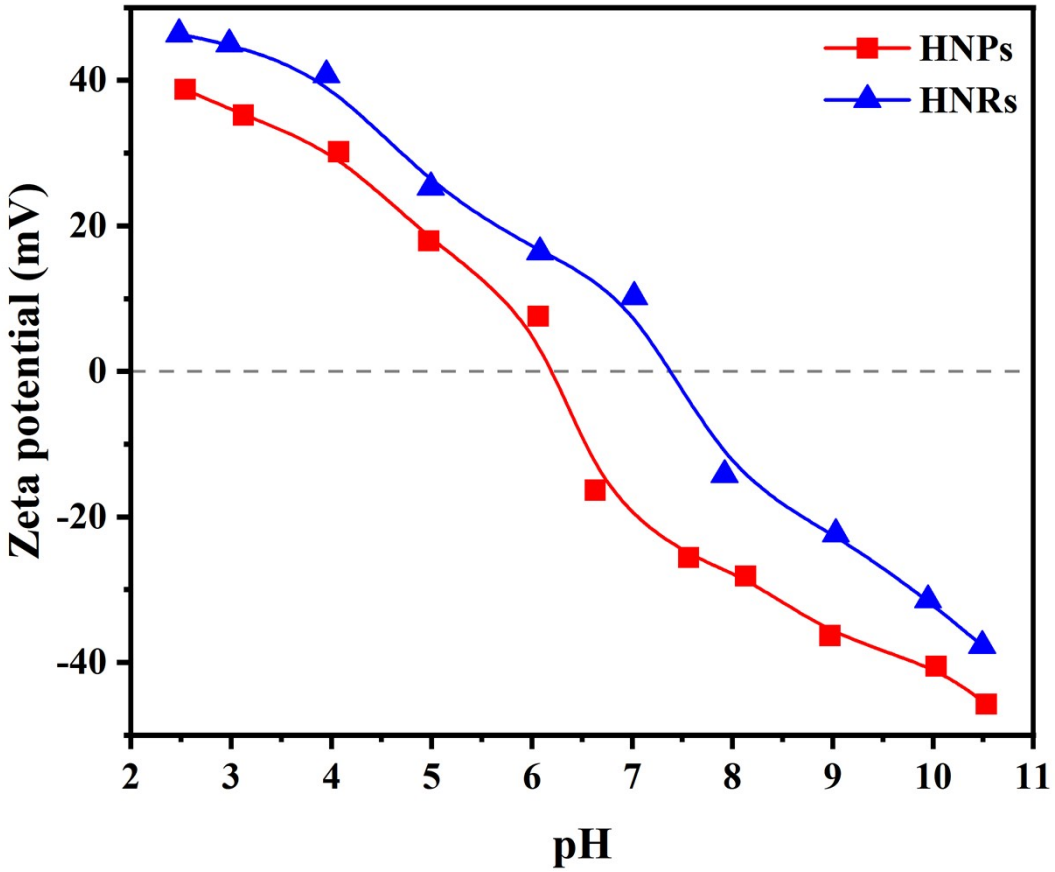

Fig. S5 Zeta potentials of HNPs and HNRs.

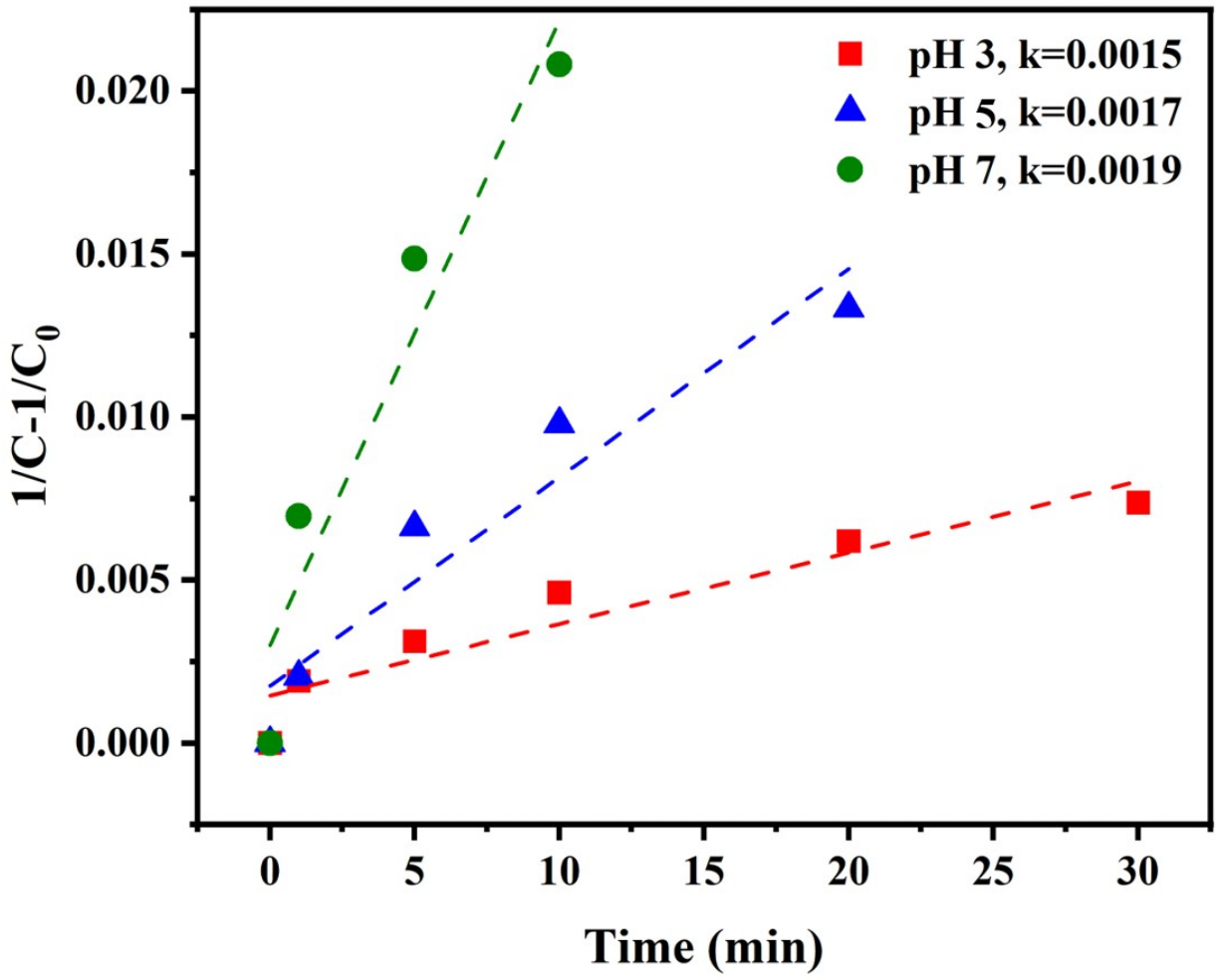

Fig. S6 Second-order kinetic model fitting for Cr(VI) and Fe(II) redox reaction at different pH.

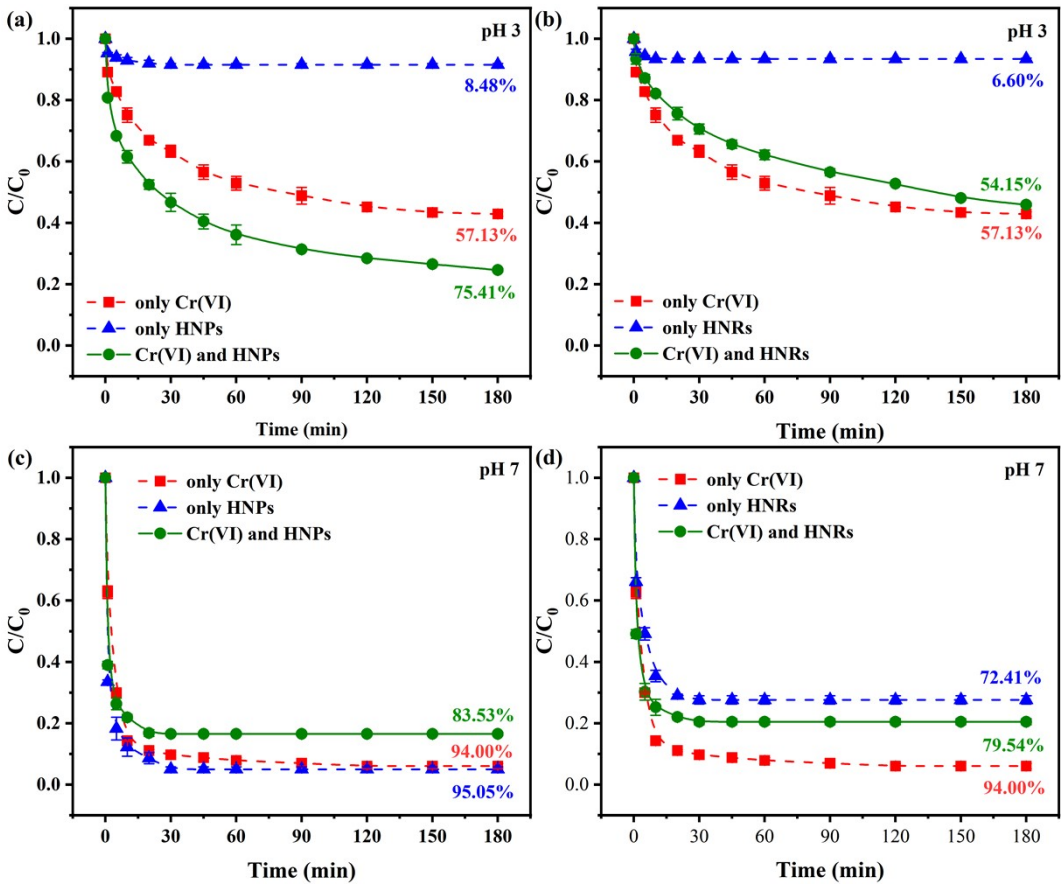

Fig. S7 Concentration of Fe(II) under (a, b) pH 3 and (c, d) pH 7 conditions with only Cr(VI) or (a, c) HNPs or (b, d) HNRs and in the presence of both. The initial concentration of Fe(II) and Cr(VI) was 20 μM, the dosage of hematite was 0.5 g/L, the ionic strength was 10 mM NaCl.

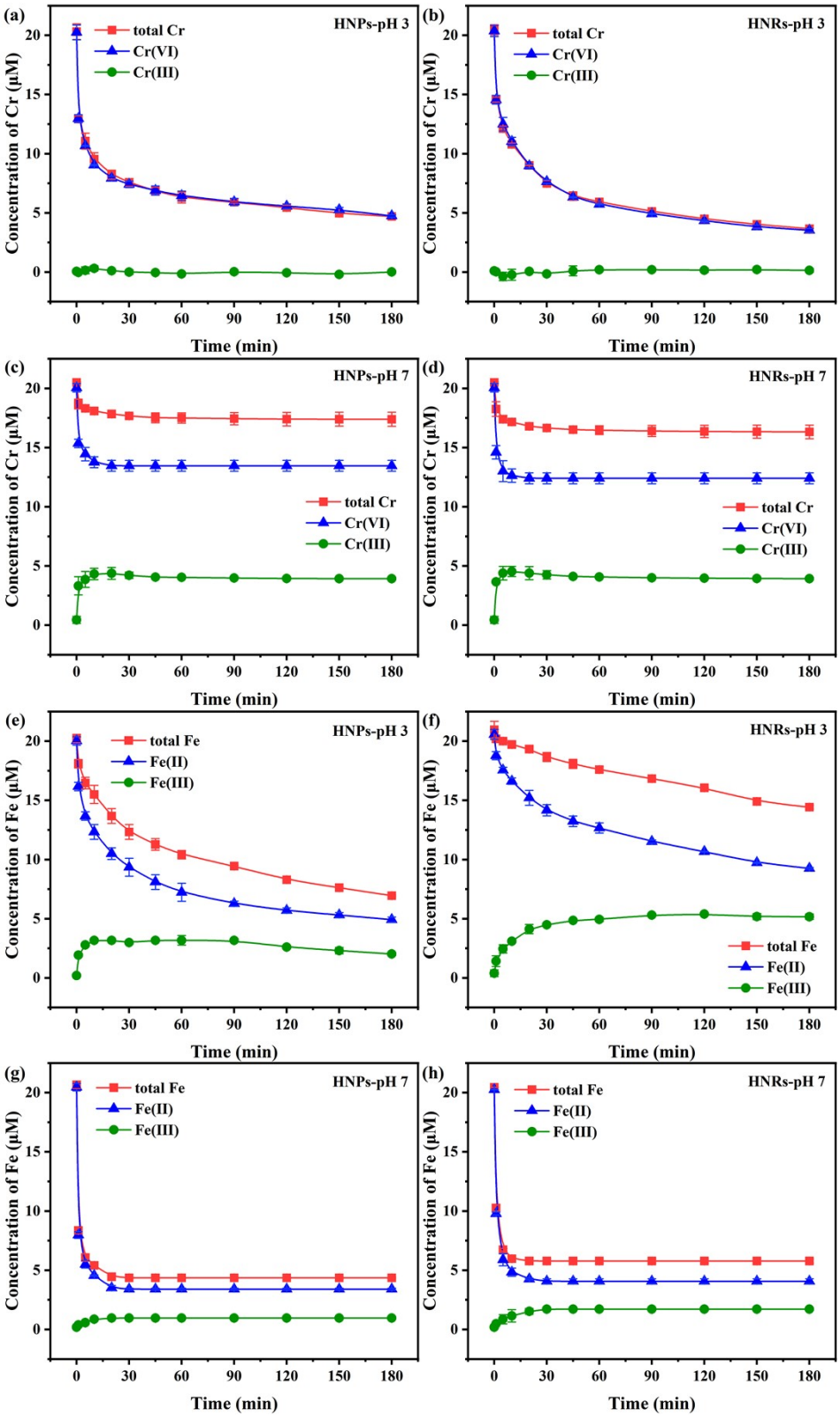

Fig. S8 Concentration changes of Cr (a-d) and Fe (e-h) in ternary systems. The initial concentration of Fe(II) and Cr(VI) was 20 μM, the dosage of hematite was 0.5 g/L, the ionic strength was 10 mM NaCl.

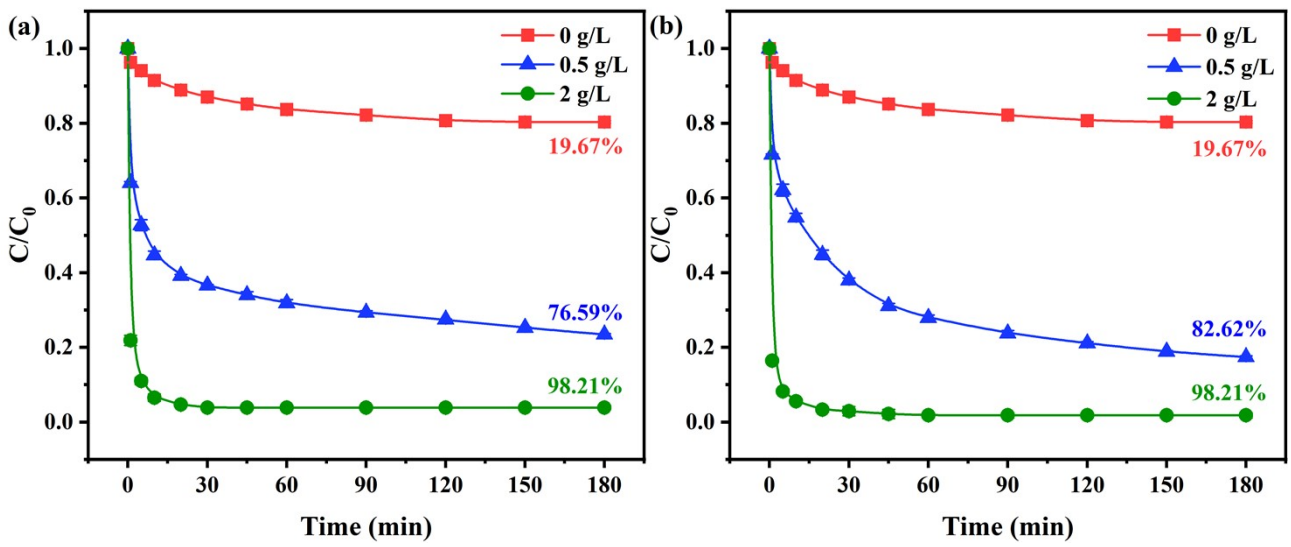

Fig. S9 Removal kinetics of Cr(VI) by different concentrations of (a) HNPs and (b) HNRs coupled to Fe(II). The initial concentration of Fe(II) and Cr(VI) was 20 μM, the dosage of hematite was 0-2 g/L, the ionic strength was 10 mM NaCl, pH was 3.

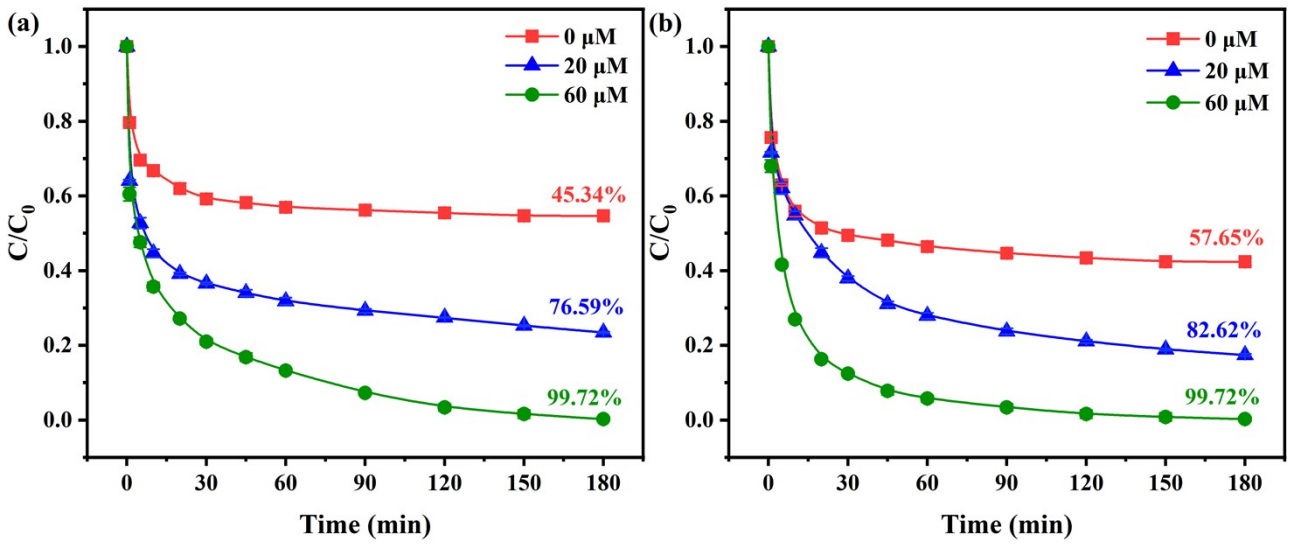

Fig. S10 Removal kinetics of Cr(VI) by (a) HNPs and (b) HNRs coupled to different concentrations of Fe(II) (0-60 μM). The initial concentration of Cr(VI) was 20 μM, the dosage of hematite was 0.5 g/L, the ionic strength was 10 mM NaCl, pH was 3.

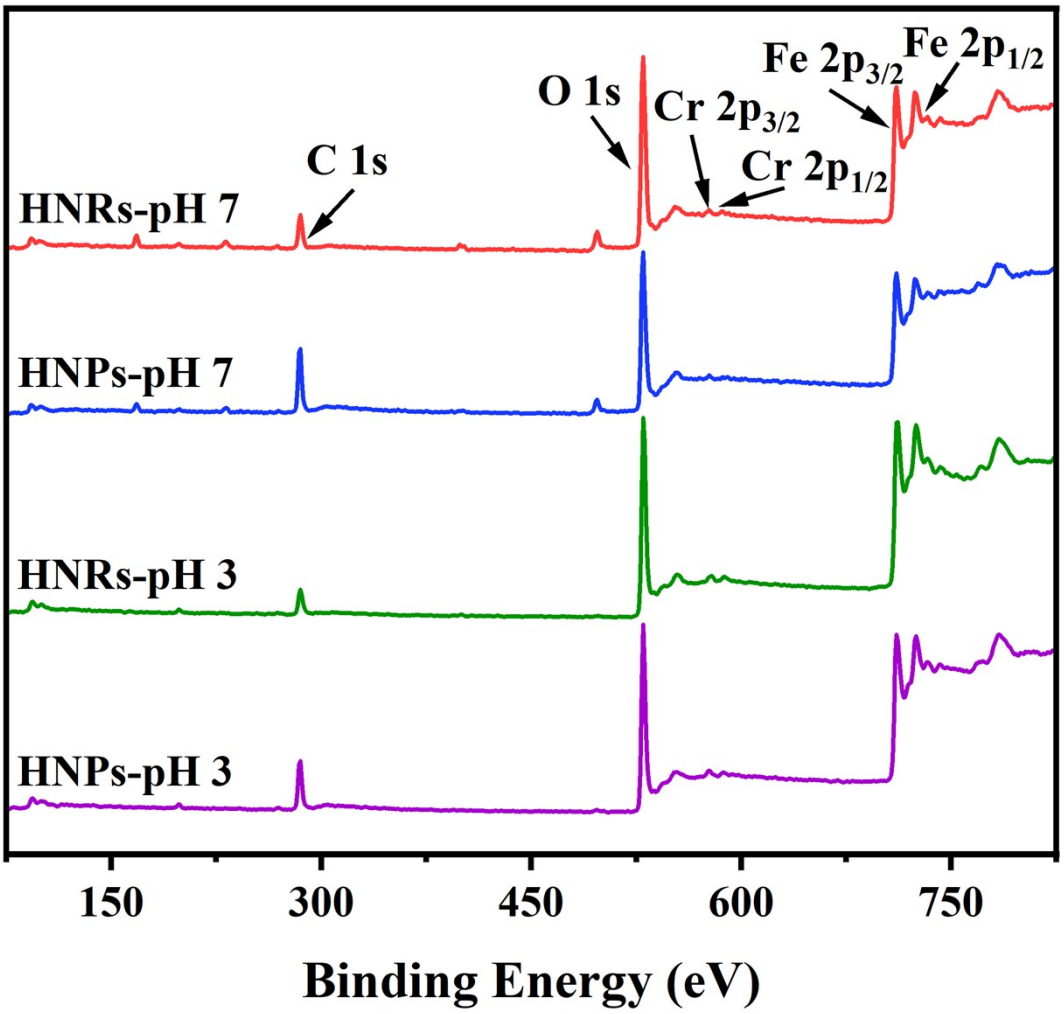

Fig. S11 XPS spectra of the reacted hematite with 20 μM Fe(II) and Cr(VI) for 180 min.

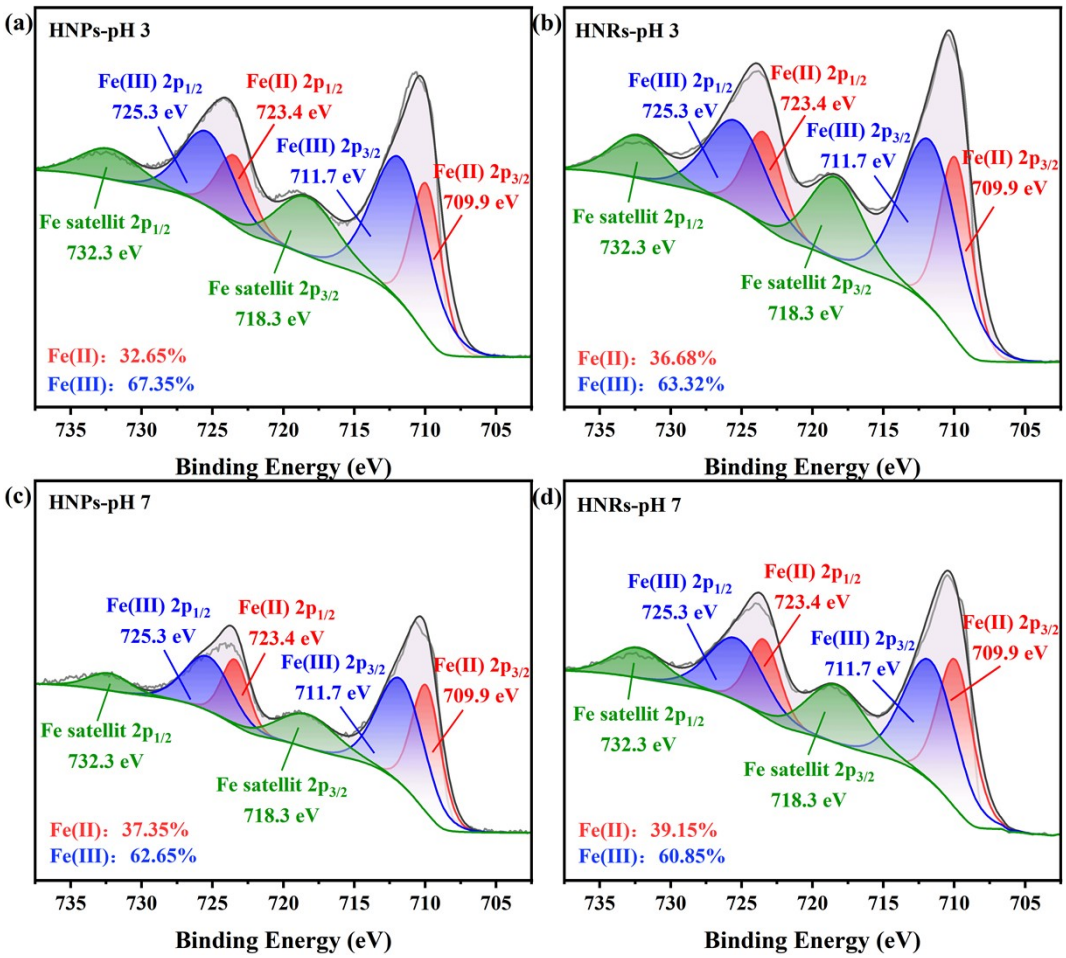

Fig. S12 Fe 2p XPS spectra of the reacted (a, c) HNPs and (b, d) HNRs with 20 μM Fe(II) and Cr(VI) under (a, b) pH 3 and (c, d) pH 7 for 180 min.

The Fe 2p could be divided into $2p_{3/2}$ orbitals of Fe(II) (709.9 eV), $2p_{3/2}$ orbitals of Fe(III) (711.7 eV), $2p_{3/2}$ orbitals of Fe satellite (718.3 eV), $2p_{1/2}$ orbitals of Fe(II) (723.4 eV), $2p_{1/2}$ orbitals of Fe(III) (725.3 eV), and $2p_{1/2}$ orbitals of Fe satellite (732.3 eV) by XPS, respectively.[2,5]

References

1 Y. Mu, Z. Ai, L. Zhang, and F. Song, Insight into Core–Shell Dependent Anoxic Cr(VI) Removal with Fe@Fe_2O_3 Nanowires: Indispensable Role of Surface Bound Fe(II), *ACS Appl. Mater. Interfaces*, 2015, **7**, 1997–2005.

2 W. Shen, Y. Mu, T. Xiao, and Z. Ai, Magnetic Fe_3O_4–FeB nanocomposites with promoted Cr(VI) removal performance, *Chem. Eng. J.*, 2016, **285**, 57–68.

3 Y. S. Ho and G. McKay, A Comparison of Chemisorption Kinetic Models Applied to Pollutant Removal on Various Sorbents, *Process Saf. Environ. Prot.*, 1998, **76**, 332–340.

4 I. J. Buerge and S. J. Hug, Kinetics and pH Dependence of Chromium(VI) Reduction by Iron(II), *Environ. Sci. Technol.*, 1997, **31**, 1426–1432.

5 M. C. Biesinger, B. P. Payne, A. P. Grosvenor, L. W. M. Lau, A. R. Gerson, and R. St. C. Smart, Resolving surface chemical states in XPS analysis of first row transition metals, oxides and hydroxides: Cr, Mn, Fe, Co and Ni, *Appl. Surf. Sci.*, 2011, **257**, 2717–2730.